

# Robust Position Control of an Electromechanical Actuator for Automotive Applications

Markus Reichhartinger and Martin Horn

**Abstract**—In this paper, the position control of an electronic throttle actuator is outlined. The dynamic behavior of the actuator is described with the help of an uncertain plant model. This motivates the controller design based on the ideas of higher-order sliding-modes. As a consequence anti-chattering techniques can be omitted. It is shown that the same concept is applicable to estimate unmeasurable signals. The control law and the observer are implemented on an electronic control unit. Results achieved by numerical simulations and real world experiments are presented and discussed.

**Keywords**—higher order sliding-mode, throttle actuator, electromechanical system, robust and nonlinear control.

## I. INTRODUCTION

Throttle actuators are placed in the intake manifold of gasoline engines. With the help of the throttle plate the airflow ratio entering the combustion chamber can be adjusted, see e.g. [1]. In the past, the throttle plate position was solely influenced by the driver. This was realized by a bowden cable mounted between the accelerator pedal and the throttle actuator. In order to implement modern driver assistance concepts such as cruise control and adaptive cruise control the mechanical throttle actuator has to be replaced by an electromechanical one, see Fig. 1. It is equipped with a dc-motor driven by an

plate position  $\varphi$  tracks a reference signal  $r$ . Existing strategies are presented in e.g. [2]–[6]. In [2] a gain scheduling PID controller, based on a linear model is proposed. In order to ensure the desired closed loop performance in the whole range of operation an adaption of the controller parameters is necessary. Paper [3] discusses a sliding-mode approach for the position control of the throttle actuator. As in the present paper the plant model is of 3<sup>rd</sup> order. The proposed observer is designed to estimate the full state. In contrast to the approach in [3] it is shown here that the implementation of an observer of 2<sup>nd</sup> order is sufficient. Besides, the approach in [3] requires chattering suppression techniques. A PID based method extended with a friction compensation is focused in [4]. In [5] a higher-order sliding-mode control strategy is applied. The required estimation is based on the time differentiation of measured signals.

The present paper is organized as follows: The modelling and the result of parameter identification of a throttle actuator is outlined in Section II. The position control concept as well as the observer design are discussed in Section III. Section IV is dedicated to the discussion of real world results, Section V concludes this paper.

## II. MODELLING OF THE ACTUATOR

Mathematical models for electromechanical throttle actuators can be found in numerous publications, e.g. [7]–[10]. In this paper a simple model for numerical simulations and for model based controller design is presented.

### A. Mathematical Model

The dc-motor represents the electrical part of the throttle actuator. It is modelled as

$$u = Ri + L \frac{di}{dt} + u_i, \quad (1)$$

where  $R$ ,  $L$  and  $i$  are the armature resistance, the inductance and the current respectively. The actuating signal is the voltage  $u$  applied to the motor. The induced voltage  $u_i$  due to the motion of the rotor is assumed to be proportional to the angular velocity  $\omega_r$  of the rotor, i.e.

$$u_i = k_m \omega_r, \quad (2)$$

where  $k_m$  is a positive constant. The motion of the throttle plate angle  $\varphi$  can be described as

$$I \frac{d^2\varphi}{dt^2} = T_s + T_f + T_m, \quad (3)$$

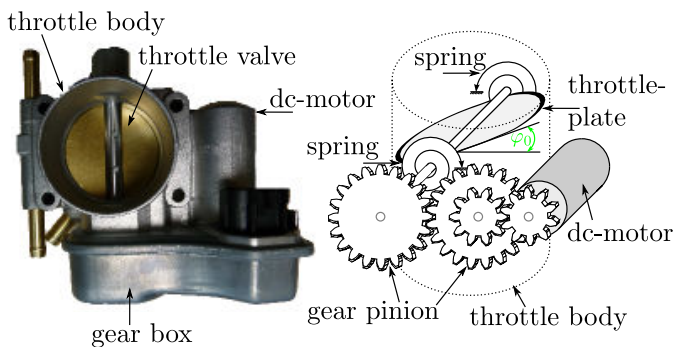


Fig. 1. Picture and sketch of the throttle actuator

engine control unit. Via a gear unit the motor is connected to the throttle plate. The rotational angle  $\varphi$  of the plate is measured with the help of two potentiometers. For safety reasons electromechanical throttle actuators are equipped with springs. In case of an electronic failure, the springs steer the plate to the so called limp home position  $\varphi_0$ . This position allows an emergency operation of the engine. The objective of the controller is to compute a motor voltage  $u$  such that the

M. Reichhartinger and M. Horn are with the Institute of Smart System-Technologies, Control- and Measurement Systems Group, Klagenfurt University, Klagenfurt, Austria, e-mail: markus.reichhartinger@uni-klu.ac.at.

where  $I$  is the moment of inertia with respect to the rotational axis of the plate. It is composed of the moment of inertia  $I_m$  of the dc-motor and the throttle plate  $I_p$ , i.e.

$$I = \eta^2 I_m + I_p, \quad (4)$$

where  $\eta$  is the gear ratio. The right hand side of (3) represents the torques acting on the valve plate. The torque introduced by the springs reads as

$$T_s = -c(\varphi - \varphi_0) - T_0 \text{sign}(\varphi - \varphi_0), \quad (5)$$

where the positive constant  $T_0$  denotes a torque due to the prestressed springs which are assumed to be linear springs with constant  $c$ , see e.g. [11]. The torque  $T_f$  considers the friction of the system and is regarded as a combination of Coulomb and viscous friction. Note that in some publications complex friction models are proposed, see e.g. [12]. Hence, it is given by

$$T_f = -T_c \text{sign}(\omega) - k_v \omega, \quad (6)$$

where  $T_c$  and  $k_v$  are positive constants. The angular velocity  $\omega$  of the throttle plate is related to the velocity  $\omega_r$  of the rotor via

$$\omega = \frac{\omega_r}{\eta} = \frac{d\varphi}{dt}. \quad (7)$$

The torque introduced by the dc-motor is modelled as

$$T_m = \eta k_m i. \quad (8)$$

Hence, equation (3) can be split up into the following first-order differential equations

$$\frac{d\varphi}{dt} = \omega, \quad (9a)$$

$$\frac{d\omega}{dt} = \frac{1}{I} \left[ -T_0 \text{sign}(\varphi - \varphi_0) - c(\varphi - \varphi_0) - T_c \text{sign}(\omega) - k_v \omega + \eta k_m i \right]. \quad (9b)$$

Using the abbreviations

$$\alpha = \frac{c}{I}, \quad \beta = \frac{M_0}{I}, \quad \gamma = \frac{k_v}{I}, \quad \delta = \frac{T_c}{I}, \quad \epsilon = \frac{\eta k_m}{I}$$

as well as equation (1) and system (9) the dynamic plant model of the throttle actuator is represented by

$$\frac{d\varphi}{dt} = \omega, \quad (10a)$$

$$\frac{d\omega}{dt} = -\alpha(\varphi - \varphi_0) - \beta \text{sign}(\varphi - \varphi_0) - \gamma \omega - \delta \text{sign}(\omega) + \epsilon i, \quad (10b)$$

$$\frac{di}{dt} = -\frac{R}{L}i - \frac{k_m \eta}{L} \omega + \frac{1}{L}u. \quad (10c)$$

### B. Parameter Identification

Plant model (10) has 11 parameters which have to be identified, see Table I. The parameters of the electrical part of throttle actuator as well as the moments of inertia and the gear ratio are typically provided by the manufacturer<sup>1</sup>. The

<sup>1</sup>Manufacturer of the throttle actuator considered in this article: Pierburg; This throttle actuator is installed in a numerous of cars, e.g. OPEL VECTRA B Caravan 1.6 i 16V, year: 11.1996-07.2002

TABLE I  
 PARAMETER OF THE THROTTLE ACTUATOR

parameter	value	unit
$R$	1.27	$\Omega$
$L$	$75 \cdot 10^{-3}$	$H$
$k_m$	0.02	$V s \text{rad}^{-1}$
$I_m$	$3.817 \cdot 10^{-6}$	$kg m^2$
$I_p$	$53.42 \cdot 10^{-6}$	$kg m^2$
$\eta$	16	-
$\alpha$	58.37	$s^{-2}$
$\beta$	267.52	$rad s^{-2}$
$\gamma$	[9 30]	$s^{-1}$
$\delta$	[65 80]	$rad s^{-2}$
$\varphi_0$	0.21	$rad$

remaining parameters are found via well known identification procedures, see e.g. [9]. The parameters  $\gamma$  and  $\delta$  corresponding to the effect of friction play a crucial role. The identification procedures only provide intervals for the values of these parameters, see Table I. Therefore the parameters  $\gamma$  and  $\delta$  are assumed to be uncertain plant parameters with nominal values

$$\gamma_0 = 19.5 \quad \text{and} \quad \delta_0 = 72.5 \quad (11)$$

chosen as the mean values of the bounds of the identified intervals. In Fig. 2 a comparison of the results achieved with real world experiment and numerical simulation are depicted. The simulation results are based on model (10), the plant parameters listed in Table I and the nominal parameters are given in equation (11). Fig. 2(a) shows the actuating signal  $u$  whereas Fig. 2(c) and Fig. 2(b) show the measured and the simulated plate position and current signal. Fig. 2(d) demonstrates that the throttle actuator is a system with hysteresis.

### III. CONTROL CONCEPT

The design of the controller is based on a model with neglected dynamics of the dc-motor. Considering the assumption  $L \approx 0$  equation (1) simplifies to

$$i = \frac{1}{R}(u - k_m \eta \omega). \quad (12)$$

Introducing a state vector  $\mathbf{x}$  composed of the position error and the velocity error, i.e.

$$\mathbf{x} = \left[ x_1 \quad x_2 \right]^T = \left[ \varphi - r \quad \omega - \frac{dr}{dt} \right]^T \quad (13)$$

the controller design model is given by

$$\frac{dx_1}{dt} = x_2 \quad (14a)$$

$$\frac{dx_2}{dt} = f(\mathbf{x}) + g u + \Delta(\mathbf{x}) - \frac{d^2 r}{dt^2}, \quad (14b)$$

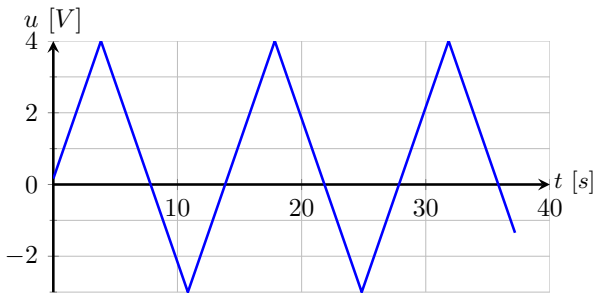
where the functions

$$f = -\alpha(x_1 + r - \varphi_0) - \beta \text{sign}(x_1 + r - \varphi_0) - \left(x_2 + \frac{dr}{dt}\right) \left(\gamma_0 + \frac{\epsilon k_m \eta}{R}\right) - \delta_0 \text{sign}\left(x_2 + \frac{dr}{dt}\right) \quad (15a)$$

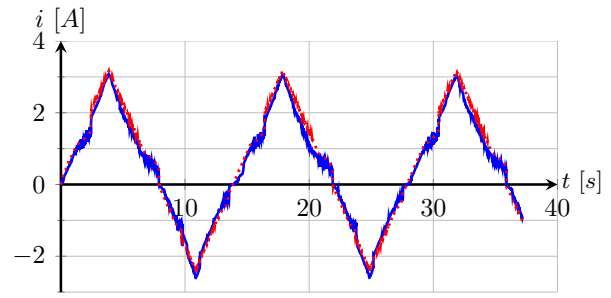
and

$$g = \frac{\epsilon}{R} \quad (15b)$$

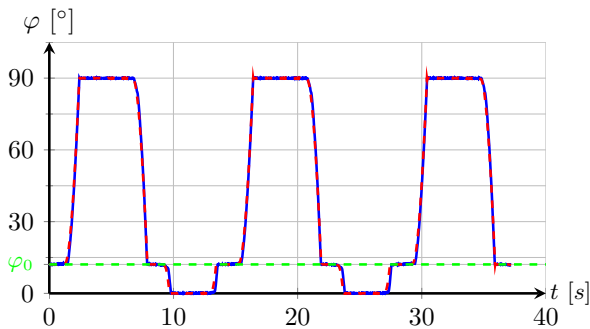
— experiment - - - simulation



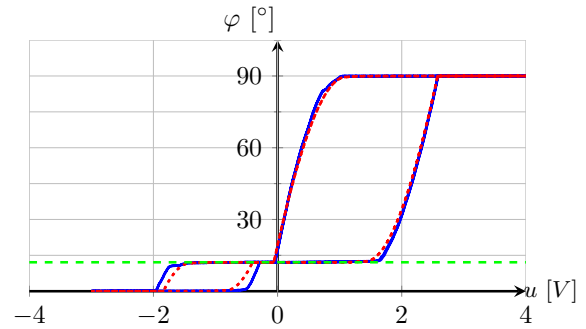
(a) Chosen actuating signal  $u$  in order to evaluate plant model (10) and its identified parameters, see Table I.



(b) Measured and simulated current  $i$  of the dc motor of the throttle actuator.



(c) Measured and simulated plate angle position  $\varphi$ . The depicted result emphasizes the influence of the limp home position  $\varphi_0$ .



(d) The throttle actuator is a system with hysteresis.

Fig. 2. Comparison of real world measurements and results achieved by numerical simulation. The numerical simulation is based on the parameters listed in Table I and the nominal parameters given in equation (11).

are assumed to be known exactly. The uncertainty  $\Delta(\mathbf{x})$  is represented by

$$\Delta(\mathbf{x}) = -\Delta_\delta - \left(x_2 + \frac{dr}{dt}\right) \Delta_\gamma, \quad (16)$$

where the uncertain parameters  $\Delta_\delta$  and  $\Delta_\gamma$  are defined as

$$\Delta_\gamma = \gamma - \gamma_0 \quad \text{and} \quad \Delta_\delta = \delta - \delta_0 \quad (17)$$

with

$$\Delta_\gamma \in [-10.5 \ 10.5] \quad \text{und} \quad \Delta_\delta \in [-7.5 \ 7.5]. \quad (18)$$

Furthermore it is assumed that the uncertainty  $\Delta(\mathbf{x})$  and the actuating signal are bounded, i.e.

$$|\Delta(\mathbf{x})| \leq \Delta_{\max} < \infty \quad \text{and} \quad |u(t)| \leq U_{\max} \leq 10V \quad \forall t. \quad (19)$$

### A. Controller Design

For the control of the uncertain plant model a sliding-mode controller based on the definition of a sliding-function

$$\sigma_1 = x_2 + h x_1 \quad \text{with} \quad h > 0 \quad (20)$$

is suggested, see e.g. [13]. Using the well known super-twisting algorithm given by

$$u = -\kappa_1 \sqrt{|\sigma_1|} \text{sign}(\sigma_1) - \kappa_2 \int_0^t \text{sign}(\sigma_1) d\tau \quad (21)$$

with  $\kappa_1, \kappa_2 > 0$

the closed loop system consisting of plant (14) and control law (21) is represented by

$$\frac{d\sigma_1}{dt} = \sigma_2 - \frac{\kappa_1}{g} \sqrt{|\sigma_1|} \text{sign}(\sigma_1), \quad (22a)$$

$$\frac{d\sigma_2}{dt} = \frac{d\Delta\sigma_2}{dt} - \frac{\kappa_2}{g} \text{sign}(\sigma_1), \quad (22b)$$

where the functions

$$\sigma_2 = \Delta\sigma_2 - \frac{\kappa_2}{g} \int_0^t \text{sign}(\sigma_1) d\tau \quad \text{and} \quad (23)$$

$$\Delta\sigma_2 = f - \frac{d^2r}{dt^2} + \Delta + h x_2, \quad (24)$$

are considered, see e.g. [14]–[16]. It is well known that the solution of system (22) converges in a finite time, if the condition<sup>2</sup>

$$\left| \frac{d\Delta\sigma_2}{dt} \right| < \infty \quad (25)$$

holds [18]. Since control law (21) requires the velocity error  $x_2$ , the estimation of the angular velocity is required<sup>3</sup>.

<sup>2</sup>This condition can serve as a basis for estimating the finite convergence time, see e.g. [17].

<sup>3</sup>In some articles the computation of  $x_2$  is realized by numerical time differentiation of the position error  $x_1$ .

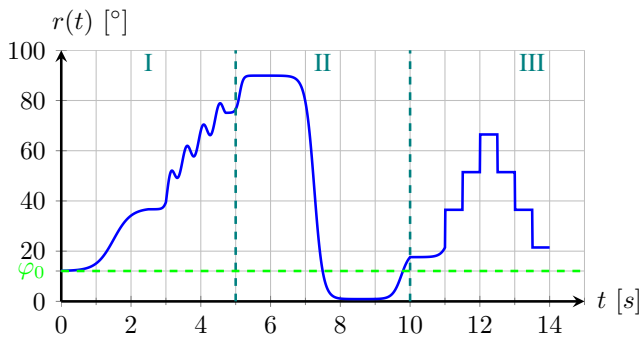


Fig. 3. Reference signal  $r(t)$  used for numerical simulation and for real world experiments.

### B. Observer Design

The design of the observer is based on the description of the throttle actuator with neglected dynamics of the dc-motor, i.e.

$$\frac{d\varphi}{dt} = \omega, \quad (26a)$$

$$\frac{d\omega}{dt} = f(\varphi - r, \omega - \dot{r}) + g u. \quad (26b)$$

As the control law design in section III-A the observer design is based on an uncertain model. This motivates the choice of a sliding-mode observer, see e.g. [17], [19], [20]. The observer is suggested as

$$\frac{d\hat{\varphi}}{dt} = \omega + \kappa_3 \sqrt{|\varphi - \hat{\varphi}|} \text{sign}(\varphi - \hat{\varphi}), \quad (27a)$$

$$\frac{d\hat{\omega}}{dt} = f(\hat{\varphi} - r, \hat{\omega} - \dot{r}) + g u + \kappa_4 \text{sign}(\varphi - \hat{\varphi}), \quad (27b)$$

where  $\kappa_3$  and  $\kappa_4$  are positive constants. Using the estimation errors

$$e_1 = \varphi - \hat{\varphi} \quad \text{and} \quad e_2 = \omega - \hat{\omega} \quad (28)$$

the estimation error dynamics is given by

$$\frac{de_1}{dt} = e_2 - \kappa_3 \sqrt{|e_1|} \text{sign}(e_1), \quad (29a)$$

$$\frac{de_2}{dt} = \hat{\Delta}(\varphi, \omega, \hat{\varphi}, \hat{\omega}) - \kappa_4 \text{sign}(e_1). \quad (29b)$$

Furthermore, it is assumed that the condition

$$\left| \hat{\Delta}(\varphi, \omega, \hat{\varphi}, \hat{\omega}) \right| = \left| f(\varphi - r, \omega - \dot{r}) - f(\hat{\varphi} - r, \hat{\omega} - \dot{r}) \right| < \infty \quad (30)$$

holds. Note, that systems (22) and (29) are of the same structure. Hence, convergence conditions and estimation of convergence time explained in e.g. [14] are applicable.

### IV. EXPERIMENT

Initial parameters for control law (21) and observer (27) are obtained by numerical simulation. The signal depicted in Fig. 3 serves as reference signal  $r$ . The reference signal consists of three sections, denoted by *I*, *II*, and *III*. Section *I* is dedicated to demonstrate the tracking performance for small changes in the reference plate angle. This indicates the

TABLE II  
CONTROLLER AND OBSERVER PARAMETERS

parameter	value	parameter	value
$h$	50	$\kappa_3$	12
$\kappa_1$	0.4	$\kappa_4$	8
$\kappa_2$	9		

ability of the feedback loop to cope with friction. The tracking performance for large changes in the reference plate angle at high angular velocities and the steady-state behavior are focused in Section *II* of the reference signal. The control algorithm is evaluated in case of discontinuous reference signals in Section *III*, see [5]. The control law and the observer are realized on a control unit with 1ms sampling time. The plate position signal is quantized with a 10 bit analog to digital converter. The power supply of the dc-motor is realized with the help of a pulse width module with constant switching frequency of 3.3kHz. The required time differentiation of the reference signal  $r$  is realized with the help of so-called robust exact differentiators, see [5], [21], [22]. Results of real world experiment and simulation achieved with parameters listed in Table II are shown in Fig. 4. The tracking performance reveals satisfactory behavior of the closed loop system, consisting of controller, observer and plant. The consistency of simulated and measured actuating signal is outstanding. Note, that neither in simulation nor in the real world experiment an anti-chattering method is implemented, see [13].

### V. CONCLUSION

Second-order sliding-mode concepts are used to realize a position control loop and an observer for an electronic throttle valve. An uncertain plant model serves as design model for controller and observer. The uncertainty results from plant parameter variations and from neglected dynamic effects. In order to obtain an initial setting for controller and observer parameters numerical simulations are carried out. The proposed concepts are implemented on an electronic control unit. The results of simulation and real world experiments are discussed and compared.

### REFERENCES

- [1] T. Aono and T. Kowatari, "Throttle-control algorithm for improving engine response based on air-intake model and throttle-response model," *IEEE Transactions on Industrial Electronics*, vol. 53, no. 3, pp. 915–921, June 2006.
- [2] M. Corno, M. Tanelli, S. Savaresi, and L. Fabbri, "Design and validation of a gain-scheduled controller for the electronic throttle body in ride-by-wire racing motorcycles," *Control Systems Technology, IEEE Transactions on*, vol. 19, no. 1, pp. 18–30, Jan. 2011.
- [3] O. Dagzi, Y. Pan, and U. Ozguner, "Sliding mode control of electronic throttle valve," in *Proceedings of the American Control Conference*, 2002, pp. 1996–2001.
- [4] J. Deur, D. Pavković, N. Perić, M. Jansz, and D. Hrovat, "An electronic throttle control strategy including compensation of friction and limp-home effects," *IEEE Transactions on Industry Applications*, vol. 40, pp. 821–834, 2004.
- [5] M. Reichhartinger and M. Horn, "Application of higher order sliding-mode concepts to a throttle actuator for gasoline engines," *IEEE Transactions on Industrial Electronics*, vol. 56, no. 9, pp. 3322–3329, Sept. 2009.

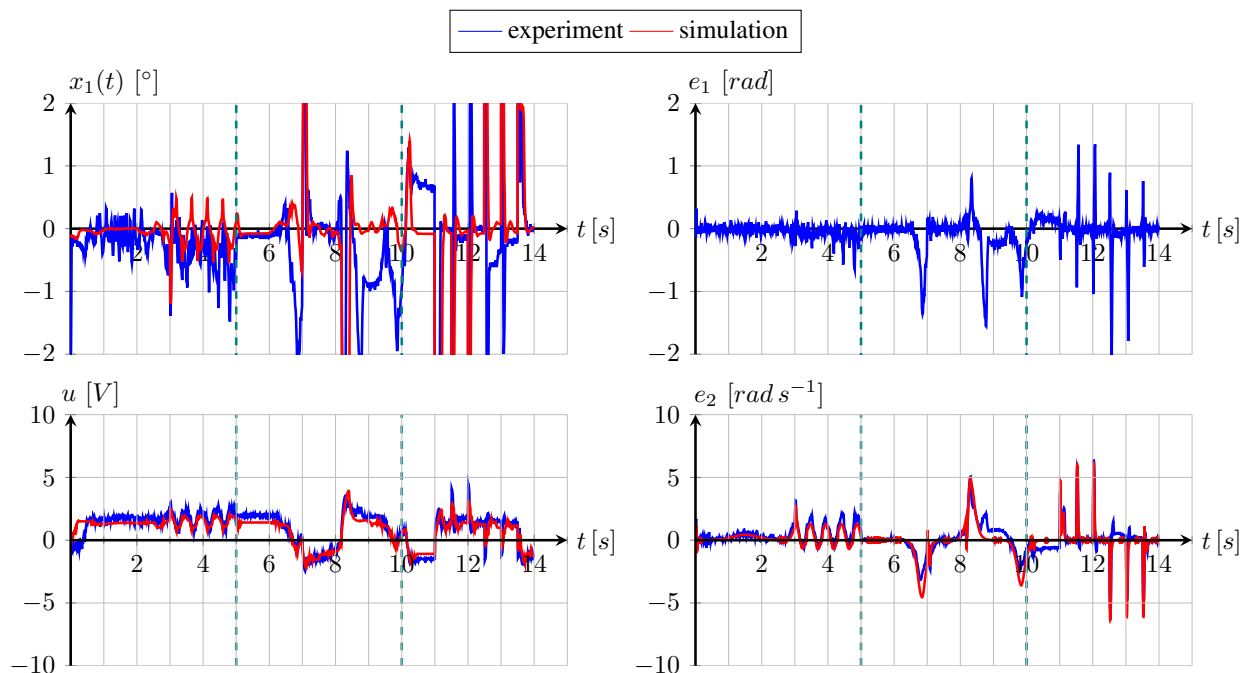


Fig. 4. Results of numerical simulation and real world experiments of the electronic throttle actuator achieved with the discussed position control strategy. The angular velocity  $\omega$  of the valve plate is estimated with the help of a second order sliding-mode observer.

- [6] D. Pavković, J. Deur, M. Jansz, and N. Perić, "Adaptive control of automotive electronic throttle," *Control Engineering Practice*, vol. 14, pp. 121–136, 2006.
- [7] K. Nakano, U. Sawut, K. Higuchi, and Y. Okajima, "Modelling and observer-based sliding-mode control of electronic throttle systems," *Transactions on Electrical Eng., Electronics, and Communications*, vol. 4, no. 1, pp. 22–28, 2006.
- [8] R. Scattolini, C. Sivierob, M. Mazzuccoa, S. Riccia, L. Poggiob, and C. Rossi, "Modeling and identification of an electromechanical internal combustion engine throttle body," *Control Engineering Practice*, vol. 5, pp. 1253–1259, 1997.
- [9] D. Pavković, J. Deur, M. Jansz, and N. Perić, "Experimental identification of an electronic throttle body," in *Proceedings of 10th European Conference on Power Electronics and Applications*, 2003.
- [10] P. Zhang, C. Yin, and J. Zhang, "Sliding mode control with sensor fault tolerant for electronic throttle," in *Proc. IEEE International Conference on Automation Science and Engineering CASE '06*, 2006, pp. 568–573.
- [11] Y. Pan, U. Ozguner, and O. H. Dagci, "Variable-structure control of electronic throttle valve," *IEEE Transactions on Industrial Electronics*, vol. 55, no. 11, pp. 3899–3907, Nov. 2008.
- [12] M. Vasak, I. Petrovic, and N. Peric, "State estimation of an electronic throttle body," in *Proc. IEEE International Conference on Industrial Technology*, vol. 1, 2003, pp. 472–477 Vol.1.
- [13] V. Utkin, J. Guldner, and J. Shi, *Sliding Mode Control in Electromechanical Systems*. CRC Press, Taylor and Francis Group, 2009.
- [14] A. Davila, J. Moreno, and L. Fridman, "Optimal lyapunov function selection for reaching time estimation of super twisting algorithm," in *Decision and Control, 2009 held jointly with the 2009 28th Chinese Control Conference. CDC/CCC 2009. Proceedings of the 48th IEEE Conference on*, 2009, pp. 8405–8410.
- [15] J. A. Moreno, *11th IEEE Workshop on Variable Structure Systems, Plenaries and Semiplenaries*, L. Fridman, Ed., 2010.
- [16] A. Levant, "Principles of 2-sliding mode design," *Automatica*, vol. 43, no. 4, pp. 576–586, 2007.
- [17] J. Moreno and M. Osorio, "A lyapunov approach to second-order sliding mode controllers and observers," in *Decision and Control, 2008. CDC 2008. 47th IEEE Conference on*, 2008, pp. 2856–2861.
- [18] A. Polyakov and A. Poznyak, "Reaching time estimation for super-twisting second order sliding mode controller via lyapunov function designing," *Automatic Control, IEEE Transactions on*, vol. 54, no. 8, pp. 1951–1955, 2009.
- [19] S. K. Spurgeon, "Sliding mode observers: a survey," *International Journal of Systems Science*, vol. 39, pp. 751–764, 2008.
- [20] J. Davila, L. Fridman, and A. Levant, "Second-order sliding-mode observer for mechanical systems," *Automatic Control, IEEE Transactions on*, vol. 50, no. 11, pp. 1785–1789, 2005.
- [21] A. Levant, "Robust exact differentiation via sliding mode technique," *Automatica*, vol. 34, no. 3, pp. 379–384, 1998.
- [22] —, "Higher-order sliding modes, differentiation and output-feedback control," *International Journal of Control*, vol. 76, pp. 924–941, 2003.



**Markus Reichhartinger** received the Dipl.-Ing. in telematics from Graz University of Technology, Graz, Austria in 2006 and the Ph.D. in Information Technology, from Alpen-Adria University Klagenfurt, Klagenfurt, Austria in 2011. He is currently a Research Assistant for Control and Measurement Systems in the Institute of Smart System-Technologies at Alpen-Adria University Klagenfurt. His research interests include the analysis of variable structure systems, control of electrical drives and industrial applications.



**Martin Horn** received the Dipl.-Ing. and the Ph.D. in electrical engineering from Graz University of Technology, Graz, Austria, in 1992 and 1998, respectively. Until 2008 he was with the Institute of Automation and Control at Graz University of Technology, Graz, Austria. In 2008 he joined the Alpen-Adria University Klagenfurt, Klagenfurt, Austria where he is currently a Professor for Control and Measurement Systems in the Institute for Smart System-Technologies. His research interests are in the fields of variable structure systems, modeling and control of mechatronic systems and automotive control systems.